

Observational biases in flux magnification measurements

H. Hildebrandt,^{1*}

¹*Argelander-Institut für Astronomie, Auf dem Hügel 71, 53121 Bonn, Germany*

Released 2014

ABSTRACT

Flux magnification is an interesting complement to shear-based lensing measurements, especially at high redshift where sources are harder to resolve. One measures either changes in the source density (magnification bias) or in the shape of the flux distribution (e.g. magnitude-shift). The interpretation of these measurements relies on theoretical estimates of how the observables change under magnification. Here we present simulations to create multi-band photometric mock catalogues of Lyman-break galaxies in a CFHTLenS-like survey that include several observational effects that can change these relations, making simple theoretical estimates unusable. In particular, we show how the magnification bias can be affected by photometric noise, colour selection, and dust extinction. We find that a simple measurement of the slope of the number-counts is not sufficient for the precise interpretation of virtually all observations of magnification bias. We also explore how sensitive the shift in the mean magnitude of a source sample in different photometric bands is to magnification including the same observational effects. Again we find significant deviations from simple analytical estimates. We also discover a wavelength-dependence of the magnitude-shift effect when applied to a colour-selected noisy source sample. Such an effect can mimic the reddening by dust in the lens. It has to be disentangled from the dust extinction before the magnitude-shift/colour-excess can be used to measure the distribution of either dark matter or extragalactic dust. Using simulations like the ones presented here these observational effects can be studied and eventually removed from observations making precise measurements of flux magnification possible.

Key words: galaxies: photometry

1 INTRODUCTION

The magnification effect of weak gravitational lensing is being used in an increasing number of projects to study dark matter structures, ranging from galaxy halos (Scranton et al. 2005; Hildebrandt et al. 2009b; Ménard et al. 2010; Bauer et al. 2014) over groups and clusters of galaxies (Van Waerbeke et al. 2010; Hildebrandt et al. 2011; Ford et al. 2012, 2014; Umetsu et al. 2011, 2014) to the large-scale-structure of the Universe (van Waerbeke 2010; Heavens & Joachimi 2011; Morrison et al. 2012). In contrast to the widely used shear effect of weak lensing some magnification observables do not require the spatial resolution of the source galaxies used in the measurement. These flux magnification observables offer the advantage of a larger source density as well as a wider redshift range (especially higher redshifts) that can be accessed.

Theoretical modelling of these flux magnification ob-

servables relies on the knowledge of the flux distribution, hence the magnitude number-counts, of the sources, before magnification. The commonly used *magnification bias* and *magnitude shift* effects represent changes in the first two moments of this flux distribution. Most studies so far have assumed knowledge of the intrinsic flux distribution or that the observed flux distribution averaged over wide areas on the sky is an unbiased estimate of the intrinsic distribution. The observables can then be calculated from lensing theory since magnification changes this intrinsic distribution in a characteristic way.

The actual observed flux distribution, however, can be affected by a number of different systematic effects. In this paper we show that depending on the observational technique these effects can be large and render the use of the observed distribution in combination with simple analytical models inaccurate. In this paper we explore such effects with simple simulations of multi-band photometric mock catalogues and quantify their importance in realistic scenarios. We also describe a way forward to interpret flux magnification measurements in the future.

* Email: hendrik@astro.uni-bonn.de

The paper is organised as follows. We present the theoretical background and analytical modelling of the flux magnification quantities in Sect. 2. The systematic effects that we simulate are discussed in Sect. 3, and the simulations are described in Sect. 4. Results are presented in Sect. 5 and discussed in Sect. 6 before we summarise and conclude in Sect. 7.

2 THEORETICAL BACKGROUND

2.1 Magnification bias

Source samples of objects used in weak gravitational lensing studies (typically galaxies but also QSOs) are always selected on one or more observables. This is necessary to avoid regions of parameter space where the measurements are unreliable (e.g. faint magnitudes, small sizes). Magnification by gravitational lensing can change these observables, e.g. flux and size. The underlying reason for this is that lensing stretches solid angles on the sky. In combination these effects can lead to a net increase or decrease in the number of objects in a sample. This effect is called magnification bias.

The best-known example of magnification bias is the change in the number density of a magnitude-limited sample of QSOs (Scranton et al. 2005) or galaxies (Hildebrandt et al. 2009b). Magnification is pushing objects over a fixed magnitude limit. If this increase in object density is larger than the decrease due to the stretching of the sky one observes an over-density of objects in magnified regions. Otherwise one might see a decrease. Only if the intrinsic distribution (i.e. the distribution before lensing) of fluxes is shaped in such a way that it exactly compensates both effects, one does not observe a change in density.

The density change depends on the logarithmic slope α_{nc} of the differential magnitude number-counts, $n(m)$,¹ of the source sample (see also Hildebrandt et al. 2009b):

$$\alpha_{\text{nc}}(m) \equiv 2.5 \frac{d \log [n(m)]}{dm}. \quad (1)$$

For a narrow source redshift slice the shape of the number-counts is equivalent to the shape of the luminosity function.

Under magnification the number-counts are changed in the following characteristic way:

$$n(m) = \mu^{-1} n_0 [m + 2.5 \log(\mu)], \quad (2)$$

with μ being the magnification and n_0 being the intrinsic number-counts before lensing. Through Taylor expansion it can easily be shown that

$$n(m) = \mu^{\alpha_{\text{nc}} - 1} n_0(m) \approx [1 + (\alpha_{\text{nc}} - 1) \delta\mu] n_0(m), \quad (3)$$

where the approximation on the right-hand side holds in the weak lensing regime, i.e. $|\delta\mu| \equiv |\mu - 1| \ll 1$.

Using the relations in either Eq. (2) or Eq. (3) requires perfect knowledge of the number-counts. In practice the measurement of the number-counts is always affected by noise. It is usually also assumed that properties of the source sample such as their colour distribution do not change under

magnification. As we will see in the remainder of the paper these assumptions are not always justified.

In practice one needs to consider a source population within a finite magnitude interval $[m_a; m_b]$. The magnification bias then becomes a measurement of the change of the zeroth order moment of the number-counts in this interval:

$$I_0 = \int_{m_a}^{m_b} n(m) dm. \quad (4)$$

According to Eq. (3) this integrated quantity changes under magnification if $\alpha_{\text{nc}} \neq 1$.²

2.2 Magnitude shift

Instead of integrating over the number-counts as in the case of the magnification bias one can also look at changes in the higher-order moments. A measurement of the shift in the mean magnitude corresponds to detecting a change of the first moment divided by the zeroth moment:

$$\langle m \rangle = \frac{I_1}{I_0} = \frac{\int_{m_a}^{m_b} m n(m) dm}{\int_{m_a}^{m_b} n(m) dm}. \quad (5)$$

Such a change can only be detected if $\frac{d^2 \log n(m)}{dm^2} \neq 0$, i.e. if the logarithmic number-counts show some curvature over the magnitude interval under consideration. Hence, for number-counts that follow a power law with a constant slope the mean magnitude does not change under magnification.

As Ménard et al. (2010) showed the magnitude shift can be linearised and approximated in the weak lensing regime by:

$$\delta m_{\text{obs}} = \langle m \rangle - \langle m_0 \rangle = C_S \delta m_{\text{ind}}, \quad (6)$$

where δm_{obs} is the observed magnitude shift, $\delta m_{\text{ind}} = -2.5 \log \mu$ is the induced magnitude shift, and the constant C_S can be calculated:

$$C_S = 1 - \frac{1}{N_{\text{tot}}} \left\{ [n_b m_b - n_a m_a] - \langle m_0 \rangle [n_b - n_a] \right\}, \quad (7)$$

with $N_{\text{tot}} = I_0$ and $n_{a,b} \equiv n(m_{a,b})$.³ The constant C_S expresses the factor by which the observed magnitude shift of an ensemble of objects is suppressed to the (unobservable) magnitude shift of an individual object. This factor depends on the curvature of the logarithmic number-counts. It vanishes for number counts that follow a power law.

2.3 Reddening

Since gravitational lensing is fundamentally achromatic one would not expect to see a change in colour from lensing alone. It was suggested by Ménard et al. (2010) to use the difference in the magnitude shifts in different bands as an estimate of reddening due to dust that is associated with the gravitational lens.

This approach is only valid if the galaxies magnified into the sample and magnified out of the sample have the same colour distribution. In the presence of noise, non-detections

¹ Those should not be confused with the cumulative number-counts $N(m)$ often used in the literature.

² This assumes that α_{nc} is constant over the interval $[m_a; m_b]$.

³ Note that Ménard et al. (2010) use just a faint magnitude cut whereas we use a bright and a faint cut here.

in some bands, and colour pre-selection this is not always the case as we will show in the following.

If one is only interested in lensing then dust reddening represent a systematic effect that needs to be removed. However, in this paper we do not treat it as a systematic effect for two reasons. First, the other systematic effects discussed here are all observational in nature whereas the dust is an astrophysical effect that alters flux magnification observables. Secondly, one can also regard the dust reddening as the main observable exploiting the fact that the techniques described here represent unique ways to study dust on large scales. For these reasons we treat dust as an observable and not as a systematic in this paper.

3 OBSERVATIONAL EFFECTS

3.1 Incompleteness

The sources used in magnification measurements are extracted from noisy data. Whether a celestial source enters a catalogue or not depends on several factors. In optical astronomy source detection means typically a combination of a flux threshold and a surface-brightness threshold (Bertin & Arnouts 1996). At fixed flux two objects can have widely different sizes and hence different surface-brightness. Thus, when operating close to the noise limit (and one almost always has to do this in weak lensing applications to reach a sufficient source density) one will preferentially miss those objects with the lowest surface-brightness at a given flux. This is one reason for incompleteness.

In this paper we are simulating a high-redshift source sample whose galaxies are usually unresolved in ground-based data. This is a case of particular interest for magnification since it allows us to measure gravitational lensing in a regime that is not accessible by shear-based methods that rely on ellipticity measurements of well-resolved source galaxies. Since we assume that our sources are unresolved we ignore surface-brightness effects in the following. It should be noted though that this can become important for flux-magnification measurements employing lower- z source samples.

Another reason for incompleteness is photon shot noise randomly scattering objects below or above the flux/surface-brightness threshold. For a non-flat flux distribution this leads to Eddington bias (Eddington 1913; Teerikorpi 2004). Due to their larger abundance more faint objects are scattered to brighter magnitudes than vice versa. The simulations used here account for this effect by construction.

3.2 Colour selection

A major problem when measuring magnification bias is the separation of sources and lenses in redshift. If the source and lens samples overlap in redshift this will give rise to physical cross-correlations in their angular positions. These physical cross-correlations are typically much larger than the magnification bias signal one is interested in and hence one needs to carefully separate the samples in redshift to minimise this effect. Redshift separation can be achieved with different techniques, most of them involving colour cuts. Note

that separating galaxies by photo- z is not conceptually different than cutting in colour space. The photo- z method represents just a more complicated, higher-dimensional, and usually less-transparent colour-cut.

Redshift separation by colour selection makes use of the fact that different regions in colour space map to different redshift regions. Applying hard cuts in colour, however, will yield a source sample that is intrinsically different (e.g. in terms of its redshift distribution) at different fluxes due to the different noise levels. Colour space is not evenly distributed and the density of galaxies can show strong gradients. Introducing noise will asymmetrically scatter galaxies around colour space generally decreasing these gradients. Hence, a fixed colour cut will typically yield a different source sample for faint galaxies than for bright ones with the former having a wider redshift distribution (and potentially a larger number of outliers at unwanted redshifts) than the latter. Conversely, galaxies at fixed redshift will be spread out over a larger region in colour space when there is more noise so that a fixed colour cut targeting these galaxies will lose an increasing fraction of the sample for decreasing signal-to-noise ratio (S/N).

In this study we simulate source galaxies at a fixed redshift. So we ignore the effect of galaxies at other redshifts scattering into the colour selection box (i.e. the region of colour space targeted to select the source sample; see Fig. 2 of Hildebrandt et al. 2009a, for an example of such a box). However, we account for the effect of noise scattering objects out of the selection box. In this particular case - faint high- z galaxies as background sources - this is the more serious effect since our sources are noisy compared to the main sample of galaxies and the u -dropouts simulated here (see Sect. 4) are generally a very clean high-redshift sample. In more general applications both effects can be of equal importance and need to be taken into account.

4 SIMULATION SETUP

For the purpose of this work we assume a background source sample consisting of Lyman-break galaxies (LBGs, Steidel et al. 1996, 2003; Giavalisco 2002) as it was used in the flux magnification studies Hildebrandt et al. (2009b, 2011, 2013), Morrison et al. (2012), and Ford et al. (2012, 2014). Some of the selection effects studied here are particularly strong when such a colour-selected, noisy sample is used. It should be noted, however, that any faint, photo- z selected sample of background sources (like e.g. the QSOs used in Scranton et al. 2005; Ménard et al. 2010) will show similar effects since the photo- z selection is essentially a more complicated cut in multi-dimensional colour space. The LBGs used here have the advantage that the colour selection is fairly simple and transparent whereas the inner workings of a photo- z code lead to a more complicated selection that is harder and more time-consuming to simulate.

Some of the effects studied here depend on the level of noise in the data. Here we simulate a survey similar in its noise properties to the CFHTLenS data set. This five-band imaging survey carried out with MegaCam@CFHT has been extensively described in Heymans et al. (2012), Hildebrandt et al. (2012), Erben et al. (2013), and Miller et al. (2013). We take the limiting magnitudes

in the five optical bands *ugriz* from Table 1 of Erben et al. (2013).

For simplicity we assume here that we have a pure, uncontaminated source sample, i.e. all sources are at the same redshift behind the lenses. We choose the redshift of the sources to be $z = 3.2$ identical to the mean redshift of the *u*-dropouts studied in Hildebrandt et al. (2009a,b). The colour selection criteria for this sample are:

$$\begin{aligned} 1.5 &< (u - g) \\ -1.0 &< (g - r) < 1.2 \\ 1.5 \cdot (g - r) &< (u - g) - 0.75 \end{aligned} \quad (8)$$

From the CFHTLS-Deep field data (Hildebrandt et al. 2009a) we also estimate the mean colours of the LBGs in the magnitude range of interest. These data are deeper than our simulated data set (~ 2.5 mag) such that we do not expect any inaccuracies in the colour estimates due to possible non-detections, even in the *u*-band, over the magnitude range of interest. We also model the colour distribution as a multivariate Gaussian with the width in the different dimensions estimated from the same data.

We further assume that the source sample follows a Schechter luminosity function:

$$\Phi(M) = \Phi_0 \left[10^{0.4(M_* - M)} \right]^{\alpha_{\text{LF}} + 1} \cdot \exp \left[-10^{0.4(M_* - M)} \right], \quad (9)$$

with Φ_0 being the overall normalisation, M_* being the characteristic absolute magnitude, and α_{LF} being the faint-end slope. We use the parameters for the *u*-dropouts reported in van der Burg et al. (2010). The derivative of the Schechter function that is under idealised conditions directly related to the slope α_{nc} (see Eq. 1) is:

$$\frac{d\Phi}{dM} = -0.4 \ln(10) \left(\alpha_{\text{LF}} + 1 - 10^{0.4(M_* - M)} \right) \Phi(M). \quad (10)$$

Besides introducing magnification we also consider the existence of dust which can be present in lens galaxies. This can counter-act the magnification by dimming background objects and hence affects the interpretation of a magnification measurement. A Milky-Way dust extinction law by Cardelli et al. (1989) is assumed and we place the lens galaxy at a redshift of $z = 0.7$. In combination with the effective wavelength of the MegaCam@CFHT filter set this allows us to calculate the change in colour of background objects behind lenses that contain such dust.

The simulation consists of the following steps:

- The *r*-band magnitude interval of interest ($22 < r < 26.5$ in this case) is split into steps of $\Delta r = 0.001$.
- Each *r*-band magnitude bin contains 200 objects such that the each simulation contains 9×10^5 galaxies. For a limited set of parameters we also run simulations with 100 times more objects to check for possible numerical inaccuracies.
- Each bin is assigned a weight corresponding to the value of the Schechter function at this apparent *r*-band magnitude (converted to absolute magnitudes assuming a standard Λ CDM universe and a source redshift of $z = 3.2$). This ensures that all magnitudes are sampled equally well. If one just randomly picked from a realistic Schechter function one would inevitably simulate very few bright objects due to the exponential shape of that function whose value changes by

several orders of magnitude over the magnitude range considered here. In the following, all statistics will include those weights without mentioning them explicitly again.

- We consider four scenarios:

(i) Reference scenario without magnification and extinction:

$$\Phi_{\text{ref}}(M) = \Phi(M). \quad (11)$$

(ii) Scenario with magnification μ :

$$\Phi_{\mu}(M) = \frac{1}{\mu} \Phi(M + 2.5 \log_{10} \mu). \quad (12)$$

(iii) Scenario with extinction due to dust with the absorption in the *r*-band being A_r :

$$\Phi_r(M) = \Phi(M - A_r). \quad (13)$$

(iv) Scenario with magnification and extinction combined:

$$\Phi_{\mu+\tau}(M) = \frac{1}{\mu} \Phi(M + 2.5 \log_{10} \mu - A_r). \quad (14)$$

Several different values for the magnification μ as well as the dust absorption A_r are simulated. In scenario (iv) we scale the value of the absorption in the rest-frame visual, A_V , with the magnification excess $\delta\mu$:

$$A_V = c_d \delta\mu. \quad (15)$$

Subsequently we calculate the absorption in the observed-frame *r*-band, A_r , by assuming the Milky-Way extinction law mentioned above. Note that the assumption of the linear relation between A_V and $\delta\mu$ does not limit the generality of the arguments presented in this paper in any way. It is just a convenient choice to present the results and relate our findings more directly to other work.

- Magnitudes in the other bands are assigned to each *r*-band magnitude bin according to the mean colours of the LBGs in the reference survey. For scenarios that include extinction the colours are modified according to the extinction law described above.

- For scenarios that include an intrinsic distribution of colours of the LBGs, random Gaussian colour offsets are calculated for each object and added to the magnitudes.

- Random Gaussian photometric errors are added to the magnitudes of each object based on the S/N given the limiting magnitudes of the simulated survey.

- These noisy magnitudes are compared to the limiting magnitudes and all magnitudes that are fainter than the limits are considered non-detections.

- Colour selection is performed with Eq. (8) yielding the final source samples. Non-detections are used to set limits on the colour indices and also decide for those sources whether the selection criteria are satisfied or not.

These steps yield well-controlled photometric mock catalogues that can be checked for number densities, mean magnitudes, and colour shifts in the different scenarios mentioned above. These quantities can then be compared to the theoretical predictions described in Sect. 2.

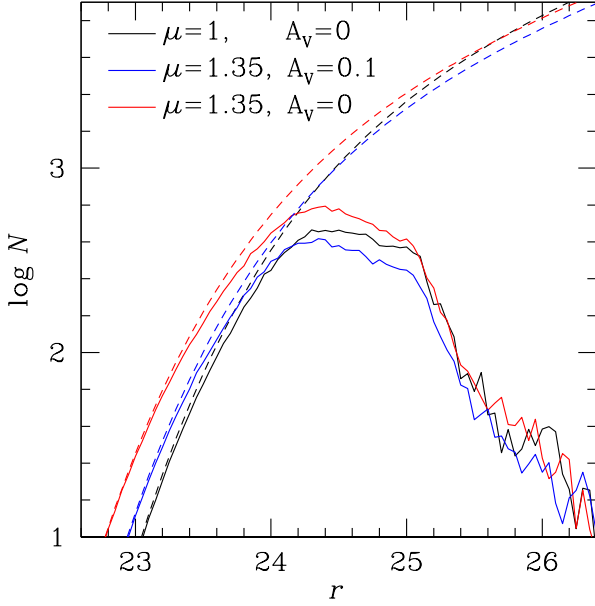


Figure 1. Number-counts of the source LBG sample in the simulations (arbitrary normalisation) as a function of r -band magnitude. The dotted lines show the intrinsic number-counts whereas the solid lines include effects from photometric noise, source detection, and colour selection. Black lines represent an un-magnified sample, red lines a sample under a magnification of $\mu = 1.35$, and blue lines a sample under a magnification of $\mu = 1.35$ as well as dust absorption by a lens galaxy at redshift $z = 0.7$ with an absorption in the rest-frame visual of $A_V = 0.1$.

5 RESULTS

5.1 Number-counts

In Fig. 1 we show the input number-counts (dotted lines) for the source sample as well as the number-counts including the effects of noise, source detection, and colour selection. Three different cases are displayed, the no-magnification and no-extinction case, the magnification-only case, and the magnification-plus-extinction case. For the setup here most of the incompleteness is caused by the colour selection. This is due to the fact that the depth of the u -, g -, and r -bands used for the colour selection of the LBGs are limiting the depth of the LBG sample more severely than the detection that is carried out in the deeper i -band. This behaviour certainly depends on the relative depths of the different bands and on the explicit form of the colour selection. Some small amount of Eddington bias from photometric noise and source detection is present in the magnitude range $25 < r < 26$. However, this Eddington bias is unimportant in practice since the depth of the u -, g -, and r -bands limits the useful magnitude range after colour selection to $r \lesssim 25$.

One important aspect apparent from this plot is the fact that the observational selection function is fixed in apparent magnitude. Although the red lines (magnification-only scenario) are shifted by more than 0.2mag horizontally⁴ with respect to the black lines (no-magnification and no-extinction)

at the bright end, the peak and the faint magnitude fall-off are almost identical magnitudes. This might seem obvious but needs to be stressed since it could potentially have an effect on how to interpret flux magnification measurements in regimes where the source sample is incomplete. In other words, the selection function is fixed in apparent magnitudes.

5.2 Magnification bias

Equation (3) relates the observed number-counts to the intrinsic number-counts via the logarithmic slope of those intrinsic number-counts, $\alpha_{nc}(m)$ (Eq. 1). Hence, the interpretation of magnification bias measurements requires a precise knowledge of this slope. As will be shown in the following there are situations where the real change in number density under magnification can differ from the theoretical expectations given in Eq. (3). This happens if effects of noise and colour selection play a role and the observed number-counts are used for measuring α_{nc} which is then used in the predictions without correcting these effects.

We define the magnification strength as

$$\Delta(m) = \left[\frac{n(m)}{n_0(m)} - 1 \right] \delta\mu^{-1}. \quad (16)$$

This quantity equals $\alpha_{nc} - 1$ in the idealised case of perfect knowledge of the number-counts and in the weak lensing regime. Figure 2 shows this magnification strength as a function of apparent r -band magnitude for magnification only (here $\mu = 1.35$; red lines) and for another scenario that also includes dust ($A_V = 0.1$; blue lines). The red solid line represents the real change in number density under magnification when all systematic effects are included. The dashed red line represent the idealised case without noise or incompleteness introduced by the object detection or colour selection. This dashed red line is barely visible because it agrees very well with the solid red line showing that the systematic effects are rather unimportant in this particular case. In different words, the incomplete sample represented by the solid red line behaves identically (within noise) to the complete sample represented by the dashed red line. This is a non-trivial result. It is not obvious from Fig. 1 that the difference (because it is a logarithmic plot) of the dashed black and red lines is the same as the difference of the solid red and black lines in that figure. This finding also means that one can get a good prediction of the magnification bias if one has access to the intrinsic number-counts and one uses the slope of those in Eq. (3).

The dot-dashed red line is the weak lensing approximation, i.e. just $\alpha_{nc} - 1$, using the slope of the intrinsic number-counts (dashed black line in Fig. 1). The difference between this weak lensing approximation and the real magnification (solid red line in Fig. 2) certainly increases for larger μ . Here we show a relatively large μ to illustrate this effect.

The dot-dashed red line in Fig. 1 assumes perfect knowledge of the intrinsic number-counts. In contrast, using the observed number-counts - uncorrected for any incompleteness - instead (i.e. using the slope of the solid black line

⁴ Note that the apparent horizontal shift is smaller than

$2.5 \log(1.35) \approx 0.33$ because of the additional suppression in vertical direction.

from Fig. 1) to estimate α_{nc} and predict the magnification strength yields the dotted red line in Fig. 1 which deviates strongly from the real situation at faint magnitudes. This means that the observed number-counts are only usable in the magnitude regime where the sample is complete and can not be used at the faint end where incompleteness sets in. This incompleteness can come from source detection, but in most practically relevant cases the incompleteness from colour selection dominates.⁵

The solid blue line shows the real $\Delta(m)$ in a scenario where the lenses also contain some dust that absorbs part of the flux. It is clear from this plot that even a moderate amount of dust in the lenses has a profound effect on the observed density change and can not be neglected when measuring magnification bias. Conversely, the dependence of the magnification bias on apparent magnitude of the background sample can be used to constrain the amount of dust in the lenses and subsequently correct the lensing measurement for extinction as was presented in Hildebrandt et al. (2013). The dashed blue line shows the density change in this scenario in the absence of noise and incompleteness. Unlike in the magnification-only scenario where the dashed and solid red lines lie exactly on top of each other, there is a significant difference between the real and idealised cases for the magnification plus dust-extinction scenario. The difference becomes important for magnitudes fainter than the peak of the number-counts (see Fig. 1). This means that the magnification bias as a function of magnitude is not just shifted to brighter magnitudes and smaller values but it actually has a different dependence on magnitude in the case with dust extinction than in the case without.

5.3 Magnitude shift

Next we explore how the theoretically calculated magnitude shift (Eq. 6) compares to the observed one in different scenarios. We are concentrating on a relatively bright *u*-dropout sample with $23 < r < 24.5$ here. This ensures that essentially all objects are detected in all bands except for the *u*-band, which makes the interpretation of the results much easier.

Figure 3 shows the observed magnitude shift as a function of the induced magnitude shift. Shown is the idealised situation without noise or colour selection. In that case the magnitude shift is achromatic so that we only show results for the *r*-band in this figure. The solid red line is the actual magnitude shift whereas the dashed black line represents the prediction from Eqs. 6 & 7 which assume the weak lensing approximation. This approximation is working extremely well for magnifications $\delta\mu \lesssim 50\%$, much better than for the magnification bias!

Figure 4 shows the magnitude shift under more realistic conditions in four different bands (i.e. the *griz*-bands, all of

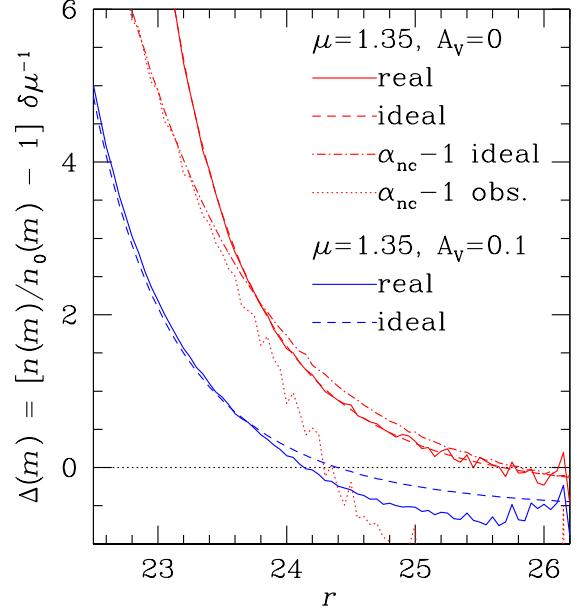


Figure 2. Magnification strength as a function of *r*-band magnitude for a magnification of $\mu = 1.35$. Shown is the ratio of the density change and the magnification excess $\delta\mu$. The dot-dashed and dotted red lines are predictions based on the weak lensing approximation estimated from the slope of the dotted and solid red curves in Fig. 1, respectively, i.e. for perfect knowledge of the intrinsic number-counts and for the observed number-counts. The dashed red line represents the magnification strength of an ideal sample, i.e. without any systematic effects, whereas the solid red line represents the magnification strength when all systematic effects are considered. The blue dashed and solid lines show the same cases for a sample that is also affected by dust absorption by a lens galaxy at redshift $z = 0.7$ with an absorption in the rest-frame visual of $A_V = 0.1$.

which are red-ward of the Lyman-break). Here noise, object detection, colour selection, and a Gaussian distribution in LBG colours are included. It is obvious that the observed magnitude shift is not fully achromatic anymore.

In particular, the magnitude shift for the *g*-band differs from the other bands by $\approx 10\%$. This is due to the fact that the colour selection in Eq. (8) depends on the *g*-band magnitude. The selection puts an upper limit on the *g* - *r* colour of $g - r \lesssim 1$, somewhat dependent on the *u* - *g* colour. In combination with the *r*-band limit of $r < 24.5$ also the *g*-band magnitude is limited. This alters the *g*-band number-counts in a characteristic way and suppresses some of the magnitude shift in that band. At the same time it slightly increases the curvature of the *r*-band number-counts.

For these reasons the theoretical prediction for the magnitude shift (represented by the dashed black line) lies in between the observed results for the *g*- and *r*-bands, with the *r*-band magnitude shift slightly enhanced and the *g*-band magnitude shift slightly suppressed with respect to the estimate. The prediction is based on the intrinsic *r*-band number-counts. Using the observed *r*-band number-counts is not a solution to correct for this bias since those are affected by incompleteness (compare the dashed and solid black lines in Fig. 1). Hence the prediction with those observed number-

⁵ This is actually a result of the typical survey design for multi-band imaging surveys. Usually one band is used as the detection band, and this band is considerably deeper than the other bands and/or taken under better observing conditions. The other bands used in the colour selection are shallower and hence introduce an incompleteness in a colour-selected galaxy sample (or in a photo-z bin).

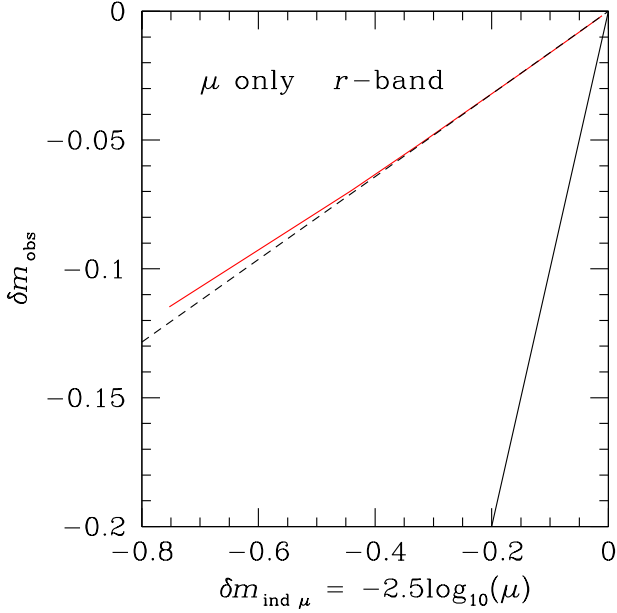


Figure 3. Observed mean magnitude shift in the r -band as a function of the induced magnitude shift for a background sample with $23 < r < 24.5$ that is not affected by any systematic effects (red solid line). The weak lensing approximation is shown by the dashed line. The solid black line is the identity relation showing the strong suppression of the observed magnitude shift compared to the induced one experienced by an individual source (but unobservable). The constant C_S corresponds to the slope of the dashed line.

counts, represented by the dotted line, greatly over-predicts the amplitude of the magnitude shift.

The case of the g -band is very different from the case of the i - and z -bands, which are not used in selecting the sample. Their number-counts are not limited in any way and they just follow the behaviour of the r -band which is used to select the sample. This is due to the fact that the $r-i$ and $r-z$ colour distributions do not change under magnification whereas the $g-r$, $g-i$, and $g-z$ colour distributions do change because of the selection effects described above.

The strength of the suppression of the g -band magnitude shift and the enhancement of the r -band magnitude shift compared to theoretical expectations depends on the exact shape of the number-counts. We tested power law distributions which theoretically should not show any magnitude shift. This still holds even for a noisy colour selected sample as the one used here. Only if there is some curvature in the logarithmic number-counts in combination with a colour selection can such a behaviour develop.

So far we looked at just magnification. If there is additional dust extinction/absorption the observed magnitude shift can not be converted into an estimate for the magnification directly. This is illustrated in Fig. 5 where variable amounts of extinction by Milky-Way like dust in a lens galaxy at $z = 0.7$ were added. The relation between observed and induced magnitude shift is very sensitive to the value of c_d (see Eq. 15) which differs for the different lines of each colour in Fig. 5. Hence in a realistic scenario the

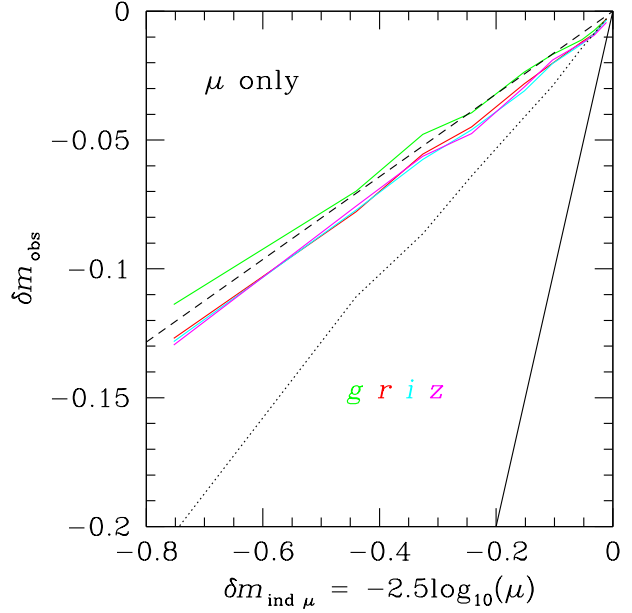


Figure 4. Same as Fig. 3 but for a real sample that is affected by all the systematic effects described in Sect. 3. The differently coloured solid lines represent the results for the different bands. The systematic effects result in a chromaticity with the observed magnitude shift depending on wavelength. The dashed line is again the prediction from weak lensing theory under the assumption of perfect knowledge of the intrinsic number-counts, whereas the dotted line represents the same prediction but using the observed number-counts.

effect of dust has to be removed before magnification can be measured with the magnitude shift.

One way of estimating and removing the effect of dust is to use colour information. In the following section we explore how well this works in the presence of selection effects.

5.4 Colour excess

Looking at the colour excess of background galaxies to estimate the amount of dust in galaxy halos along the line of sight was suggested by Ménard et al. (2010). The chromaticity of the magnitude shift induced by magnification in the presence of noise and colour selection as shown in Fig. 4 could mean that a direct estimate of the amount of dust from the colour excess might also be biased. As illustrated in Fig. 6, even without magnification, i.e. just considering dust extinction, the observed colour excess can be different from the induced colour excess. In this plot these two quantities are compared for the dust-only case. The observed colour excess in the $g-r$ colour is lower than the induced colour excess by dust extinction by about a factor of two. This is due to the systematic effects discussed above which lead to galaxies with different SEDs entering the sample than leaving the sample when extinction is present. The $g-r$ colour distribution is the only one that is limited at $g-r \lesssim 1$ because of the selection in Eq (8). The change in this distribution, which is the observable here, is slightly suppressed because of this cut in the observed colour. Interestingly, the

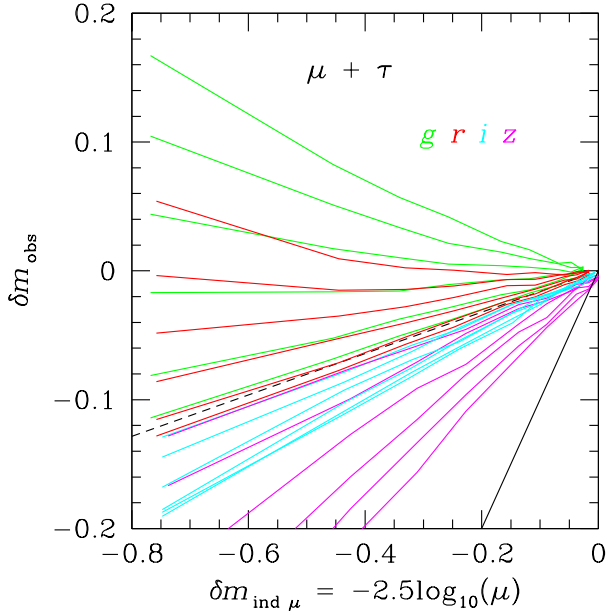


Figure 5. Same as Fig. 4 but including varying amounts of dust in a lens galaxy at redshift $z = 0.7$. It is obvious that the relationship between the induced and observed magnitude shift is extremely sensitive to the amount of dust absorption. Here we vary the scaling between the magnification excess and the absorption in the rest-frame visual, $A_V = c_d \delta\mu$. The different lines correspond to different values of $c_d = 0.0; 0.1; 0.3; 0.5; 0.7; 0.9$ going from bottom to top for the g - and r -bands and from top to bottom for the i - and z -bands, since objects are selected in r .

same behaviour is observed even if we change the shape of the r -band number-counts into a power law.

If on top of the dust extinction there is additional magnification the situation changes only slightly. As can be seen in Fig. 7 the observed colour excess in $r-i$, $r-z$, and $i-z$ is still an unbiased estimate of the induced colour excess. Due to the apparent chromaticity of the magnification-induced magnitude shift in the g -band the observed colour excess in $g-r$ depends on the amount of magnification, with the different green lines in Fig. 7 corresponding to different amounts of magnification.

The result from Fig. 7 means that one can use the $r-i$, $r-z$, and $i-z$ colour indices to directly (i.e. even in the presence of selection effects and noise) estimate the colour excess induced by dust. Assuming an extinction law (or even fitting the extinction law with multiple colour indices as it was done in Ménard et al. 2010) one can convert the colour excess into an absorption and correct the magnitude shift for dust extinction. Hence one can recover the magnification-only results from Fig. 4 by combining the measurements of Fig. 5 and Fig. 7.

6 DISCUSSION

The results discussed in this paper suggest that the interpretation of flux magnification observables under realistic conditions can be more complicated than previously thought. If effects like noise, colour selection, and dust extinction are simulated the results can differ greatly from theoretical pre-

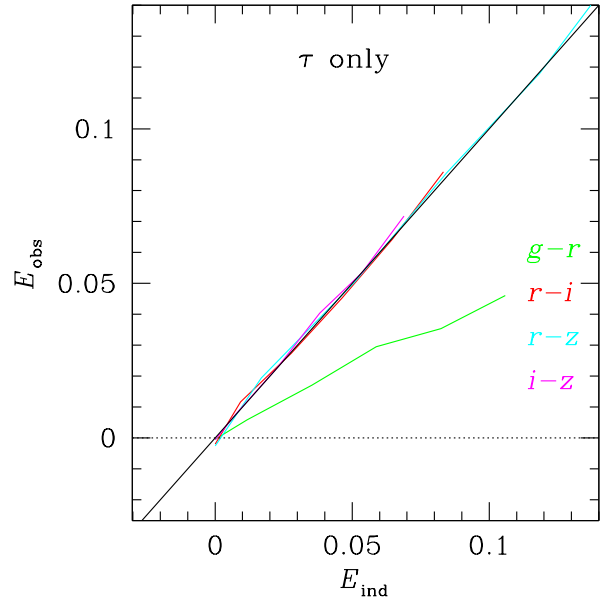


Figure 6. Observed colour excess as a function of induced colour excess for a sample that is just affected by dust and no magnification. The differently coloured lines correspond to different colour indices, and the black line is the identity relation. Whereas the observed excess in the $r-i$, $r-z$, and $i-z$ colour indices can be directly converted to the induced colour excess, the $g-r$ colour index behaves differently because of the colour selection.

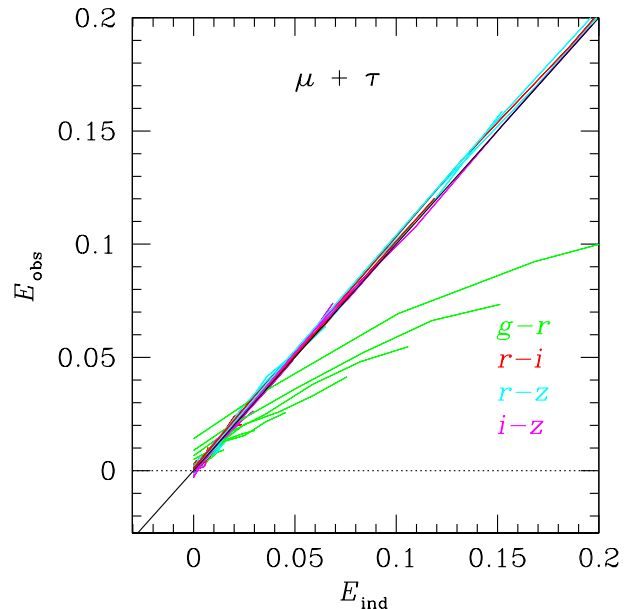


Figure 7. Same as Fig. 6 but additionally including varying amounts of magnification, $\mu = 1.01; 1.03; 1.05; 1.10; 1.15; 1.25; 1.35; 1.5; 2.0$ going from bottom to top. The observed excess in the $r-i$, $r-z$, and $i-z$ colour indices remains a reliable estimate of the induced colour excess since the relation is independent of the amount of magnification. This means that the colour excess can be converted to an absorption which can be used to correct the magnitude shift for dust effects.

dictions that ignore those effects. Here we illustrate this on a source sample that is quite sensitive to those systematic effects. In different situations these systematics could possibly be more or less important. Dedicated simulations are necessary to decide this and establish robust corrections for each flux magnification measurement.

Given the importance of dust extinction in magnification bias as well as magnitude shift measurements it is clear that any magnification study has to take dust into account. A possible way to do this is to use the colour excess from colour indices that are free from systematics (like the three redder colour indices in our example) to estimate the amount of extinction. A different and possibly complementary way would be to use the dependence of the magnification bias as a function of magnitude (Fig. 2). This technique was applied in Hildebrandt et al. (2013) and is also generally useful if colour information is unavailable or limited.

Once a robust estimate of the dust extinction is obtained one can correct magnitude shift or magnification bias measurements for this. Then one is still left with possible systematic errors from incompleteness due to colour selection or source detection. In order to account for these one has to revert to simulations. There does not seem to be a purely observational way to establish these corrections given the complexity of the data analysis involved (data reduction, source detection, multi-colour photometry, photo- z , etc.).

7 SUMMARY AND CONCLUSIONS

In this paper we simulate a high-redshift galaxy sample that has been used in many magnification studies. By controlling several systematic effects in these simulations we gain knowledge about their importance in typical flux magnification science applications. We show that the magnification bias for an incomplete sample is virtually identical to the magnification bias of a complete sample. However, an incomplete sample can not be used to estimate the slope of the magnitude number-counts which is required for any prediction of flux magnification. This estimate has to come from deeper data that are unaffected by noise in the magnitude range of interest. We also show that dust extinction can alter the magnification bias significantly and needs to be taken into account when studying sources that are magnified by lenses that potentially contain dust.

Magnitude shift measurements can become chromatic due to selection effects, even when the underlying process - gravitational lensing - is inherently achromatic. This chromaticity can mimic dust extinction and needs to be distinguished from the latter by the techniques described here. Similar to the magnification bias dust can affect the magnitude shift and its effect needs to be modelled/removed before a lensing measurement can be used to e.g. study dark matter halos.

The work presented here has potential implications for previous studies using flux magnification. We simulated a CFHTLenS-like survey with one particular source sample, $z \sim 3$ u -dropouts, and can not make strong general statements about results presented in the literature. However, it is conceivable that some of the results need to be revisited and checked for systematic effects. In the future it will be indispensable to run such simulations if magnification is go-

ing to be used as a precision tool in extragalactic astronomy alongside weak lensing shear and other techniques.

The simulations used here are based on several simplifications. In future studies these simplifications need to be dropped and the simulations made more realistic. In particular, a full redshift and SED range needs to be included and also a photo- z code needs to be run on the mock galaxies. This will then also allow galaxies at low redshift to scatter into our high-redshift source sample, an effect that was ignored here.

So far the simulations we are using are based purely on photometric mock catalogues. For some precision studies and for analysing the impact of some other systematic effects it will become necessary to also include effects of galaxy clustering, blending, etc. Such advanced mocks would have to be based on N-body simulations, possibly with ray-tracing. Such a setup would come closer to a full end-to-end treatment of magnification and this should be the long-term goal to exploit this observational technique in very large surveys like Euclid, LSST, and WFIRST.

ACKNOWLEDGEMENTS

The author would like to thank Catherine Heymans, Peter Schneider, Malte Tewes, Alan Heavens and Christopher Morrison for useful comments on the paper draft.

H. Hildebrandt is supported by an Emmy Noether grant (No. Hi 1495/2-1) of the Deutsche Forschungsgemeinschaft.

REFERENCES

- Bauer A. H., Gaztañaga E., Martí P., Miquel R., 2014, MNRAS, 440, 3701
- Bertin E., Arnouts S., 1996, A&AS, 117, 393
- Cardelli J. A., Clayton G. C., Mathis J. S., 1989, ApJ, 345, 245
- Eddington A. S., 1913, MNRAS, 73, 359
- Erben T. et al., 2013, MNRAS, 433, 2545
- Ford J., Hildebrandt H., Van Waerbeke L., Erben T., Laigle C., Milkeraitis M., Morrison C. B., 2014, MNRAS, 439, 3755
- Ford J. et al., 2012, ApJ, 754, 143
- Giavalisco M., 2002, ARA&A, 40, 579
- Heavens A. F., Joachimi B., 2011, MNRAS, 415, 1681
- Heymans C. et al., 2012, MNRAS, 427, 146
- Hildebrandt H. et al., 2012, MNRAS, 421, 2355
- Hildebrandt H. et al., 2011, ApJ, 733, L30+
- Hildebrandt H., Pielorz J., Erben T., van Waerbeke L., Simon P., Capak P., 2009a, A&A, 498, 725
- Hildebrandt H., van Waerbeke L., Erben T., 2009b, A&A, 507, 683
- Hildebrandt H. et al., 2013, MNRAS, 429, 3230
- Ménard B., Scranton R., Fukugita M., Richards G., 2010, MNRAS, 405, 1025
- Miller L. et al., 2013, MNRAS, 429, 2858
- Morrison C. B., Scranton R., Ménard B., Schmidt S. J., Tyson J. A., Ryan R., Choi A., Wittman D. M., 2012, MNRAS, 426, 2489
- Scranton R. et al., 2005, ApJ, 633, 589

- Steidel C. C., Adelberger K. L., Shapley A. E., Pettini M., Dickinson M., Giavalisco M., 2003, *ApJ*, 592, 728
- Steidel C. C., Giavalisco M., Pettini M., Dickinson M., Adelberger K. L., 1996, *ApJ*, 462, L17
- Teerikorpi P., 2004, *A&A*, 424, 73
- Umetsu K., Broadhurst T., Zitrin A., Medezinski E., Hsu L.-Y., 2011, *ApJ*, 729, 127
- Umetsu K. et al., 2014, *ApJ*, 795, 163
- van der Burg R. F. J., Hildebrandt H., Erben T., 2010, *A&A*, 523, A74
- van Waerbeke L., 2010, *MNRAS*, 401, 2093
- Van Waerbeke L., Hildebrandt H., Ford J., Milkeraitis M., 2010, *ApJ*, 723, L13